Stimulated emission of phonons in an acoustical cavity

P. A. Fokker, J. I. Dijkhuis, and H. W. de Wijn
Faculty of Physics and Astronomy, and Debye Research Institute, Utrecht University, P.O. Box 80000, 3508 TA Utrecht, The Netherlands

(Received 6 May 1996)

Stimulated emission is studied of phonons resonant with the metastable Zeeman-split $\overline{E}(^2E)$ doublet in ruby. Initial population inversion of this two-level system is prepared by selective pulsed optical pumping, and the ensuing stimulated emission of resonant phonons is observed via an accelerated growth of the luminescence intensity emanating from the lower level. Under favorable conditions, a periodic recurrence of the process of stimulated emission is observed, which points to a phonon cavity formed by the end faces of the crystal in combination with a limited interaction length of the resonant phonons. To analyze these phenomena in detail, use is made of rate equations for the phonon occupation and the level populations with explicit account of their position dependences. With plausible assumptions an analytic solution of these equations is achieved, which excellently fits the data. The effect of lattice anharmonicity is shown to depend on the phonon energy in agreement with the theoretical prediction. [S0163-1829(97)05405-2]

I. INTRODUCTION

It is well known that optical laser action can occur in a cavity containing an active population-inverted medium if the mirrors making up the cavity reflect the emitted light back into the active zone. In this paper, we report on quite a similar phenomenon for phonons in a crystalline solid. The active medium consists of a metastable population-inverted Zeeman-split spin system, with which the phonons couple via a direct spin-lattice interaction. Stimulated emission of phonons by the spin system results in a prolific rise of the phonon occupation number, which may be tracked via the associated speedup of the spin dynamics. A remarkable result of the present experiments is that the phonon occupation, once it has leveled off because the phonons have left the resonant zone, increases further following specular reflection of the phonons by the crystal boundaries after a delay equal to their round-trip time through the crystal. In other terms, the end faces of the crystal form a phonon cavity.[1] In addition, the effects of lattice anharmonicity are found to be strongly dependent on the phonon energy.

The inverted level system chosen for the present experiments is the optically excited metastable $\overline{E}(^2E)$ Kramers doublet of Cr^{3+} in a single crystal of dilute ruby Al_2O_3:Cr^{3+}, kept at a temperature below 2 K to remove thermal phonons. The inversion was created by selective population of the upper component of $\overline{E}(^2E)$ by pulsed optical pumping. More than any other system in which stimulated phonon emission has been observed[2–9] the $\overline{E}(^2E)$ doublet in ruby has been found to be extremely suited for the purpose of studying stimulated phonon emission in the regime of 0.5–5 cm^{-1}.[10] Its particular advantages include the narrow linewidth of the phonon transition connecting the $\overline{E}(^2E)$ levels ($\Delta\nu \approx 60$ MHz), the weak lattice anharmonicity, and the fact that the degree of inversion can be controlled in a simple way by adjusting the pump power. In addition, the phonon energy and the spin-phonon coupling can be chosen in a wide range of values by varying the magnetic field in strength and orientation.[11]

The theory developed below to describe the dynamics of the phonons coupled with the spin system is based on a set of incoherent equations of motion for the level populations and the occupation of the resonant phonons. The migration of the phonons through the active zone, which is an essential ingredient in the present context, is accommodated by making the equations explicitly dependent on the position and including a term dependent on the phonon group velocity. As it appears, an analytical solution can be achieved with only minor simplifications. By repetitive use, the equations furthermore account for the next passages of the phonons through the active volume after their reflection by the crystal boundaries. The equations finally permit us to include loss by upconversion in a simple way. Excellent agreement is thus obtained with the data, which cover over one decade in the phonon energy and over four decades in the spin-phonon relaxation time.

II. EXPERIMENTS

A single crystal of ruby, having a Cr^{3+} concentration of about 700 at ppm, was mounted in a cryostat with a superconducting magnet. The crystal was immersed in superfluid He at approximately 1.8 K to suppress thermal relaxation by direct phonon processes as well as thermal relaxation resulting from higher-order processes, such as Orbach and Raman processes. It measured $11\times9\times4$ mm^3, with the crystalline symmetry axis (c axis) perpendicular to the largest faces. The surfaces were polished to a roughness of 0.1 μm.

A pulsed tunable dye laser [operating with 4-dicy-ano-methylene-2-methyl-6-*p*-dimethyl-aminostyryl-4*H*-pyran (DCM)] was pumped with an excimer laser (operating with HCl-Xe), and used to selectively populate the upper componentE_+ of the Zeeman-split metastable $E(^2E)$ doublet out of the lowest sublevel ($M_S=-\frac{3}{2}$) of the $^4A_2$ ground quartet. The dye laser supplied pulses of about 10-ns duration at a repetition rate of 10 Hz and energies of up to 1

mJ. The laser beam was focused within the crystal to a waist of about 300 μm, thus effectively pumping a cylindrical excited zone oriented approximately parallel to the magnetic field. The luminescence emanating from the crystal was collected under right angles to the exciting laser beam and dispersed in a 0.8-m double monochromator to select the transition from E_- to the $M_S=+\frac{1}{2}$ sublevel of $^4A_2$. Standard time-resolved photon-counting and digital signal-averaging techniques ensured a temporal resolution of 0.1 μs. Averaging over typically 5000 traces was needed for sufficient statistics.

The Zeeman splitting of the $\overline{E}(^2E)$ state was controlled by magnetic fields of up to 6 T. The field was oriented in the horizontal plane, as was the c axis. This geometry facilitated adjustment of the angle θ between them. Combined with variation in the field, this adjustment permitted us to tune both the $\overline{E}(^2E)$ level splitting δ and the direct spin-phonon relaxation time T_1 within $\overline{E}(^2E)$ to the needs of the experiments.[11] Measurements were collected either at a constant magnetic field $H=6$ T with θ ranging from 30° to 85° or at a constant $\theta=69°$ with H ranging between 1 and 6 T. This covers a range from 0.4 up to 6.0 cm^{-1} in δ and a range from 600 ms down to 11 μs in T_1.

For the sake of an additional proof of reflection of the generated phonons by the end faces, a number of experiments were repeated for a crystal of notably different dimensions, measuring $6\times2\times2$ mm^3, with the longest dimension parallel with the magnetic field. Here, the magnetic field was fixed at 3 T and oriented at a fixed angle of 69° from the crystalline c axis. The excited zone was taken along the longest dimension of the crystal.

III. THEORY

In this section, we develop an analytical theory for the dynamics of resonant phonons emitted by stimulated emission after inversion of a two-level system. For the $\overline{E}(^2E)$ system, the typical time associated with the process of stimulated phonon emission is much longer than the time $T_2^*\sim10$ ns characterizing the inhomogeneous broadening of the spin-phonon transition. Under this condition effects of coherence may presumably be neglected, which makes possible the use of rate equations for the phonon occupation and the level populations.

As a starting point, we adopt the following equations of motion for the occupation numbers $p_{\mathbf{k}}$ of phonons of wave vector $\mathbf{k}$ and the population densities N_+ and N_- of the excited-state levels E_+ and E_-:

$$\left(\frac{\partial}{\partial t}+\mathbf{v}\cdot\nabla\right)p_{\mathbf{k}}=\frac{(p_{\mathbf{k}}+1)N_+-p_{\mathbf{k}}N_-}{\rho\Delta\nu T_1}, \tag{1}$$

$$\frac{dN_+}{dt}=-\sum_{\mathbf{k}}\frac{(p_{\mathbf{k}}+1)N_+-p_{\mathbf{k}}N_-}{\rho\Delta\nu T_1}-\frac{N_+}{\tau_R}, \tag{2}$$

$$\frac{dN_-}{dt}=\sum_{\mathbf{k}}\frac{(p_{\mathbf{k}}+1)N_+-p_{\mathbf{k}}N_-}{\rho\Delta\nu T_1}-\frac{N_-}{\tau_R}. \tag{3}$$

Equations (1)–(3), in which the summations are restricted to the resonant phonon modes, specify both the time and position dependence of N_+, N_-, and the $p_{\mathbf{k}}$. The term $\mathbf{v}\cdot\nabla p_{\mathbf{k}}$ in Eq. (1) accounts for the migration of phonons at their group velocity $\mathbf{v}$. The terms containing the direct spin-phonon relaxation time T_1 represent the dynamical interaction between the phonons and the spin system via direct processes; the parts linear in $p_{\mathbf{k}}$ refer to stimulated emission and absorption of phonons, and the remaining part to their spontaneous emission. The quantity ρ is the density of phonon modes and $\Delta\nu$ is the linewidth, and so $\rho\Delta\nu$ equals the density of phonon modes resonant with the two-level system. For a reasonable estimate of ρ, we rely on the Debye approximation, restricting ourselves to the two transverse acoustic modes ($v=6.4$ km/s) because these modes predominantly support the stimulated emission. The radiative decay back to the $^4A_2$ ground state is implemented by way of the linear loss terms with a time constant equal to the radiative lifetime $\tau_R\approx4$ ms. Note that Eq. (1) only contains the interaction of the phonons with the spin system, and so it reduces to the simple case of an undamped traveling phonon beyond resonance with the excited Cr^{3+} ions.

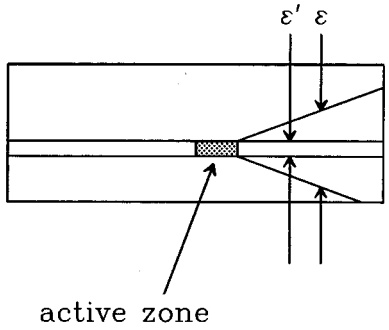

FIG. 1. Principle of the geometry. A fraction ε of the phonon modes take part in the first stage of the stimulated emission. After specular reflection, only a fraction ε' is involved in the subsequent passages through the active zone.

Because the excited zone is pencil shaped, the development of $p_{\mathbf{k}}$ by stimulated amplification is subject to substantial anisotropy. This, in fact, permits us to reduce Eqs. (1)–(3) to a set of one-dimensional equations. Indeed, phonons propagating along the cylinder axis need a much longer time to escape out of the active zone than do phonons traveling at right angles. In the latter case, the interaction length is limited to the radius of the pencil, which is about 150 μm. For phonons traveling along the axis, experiments by us[12,13] have shown that macroscopic inhomogeneities in the resonance frequency cause the amplified phonon packet to become off resonance after traveling over a distance of typically 600 μm, which corresponds to a time available for interaction of the order of 100 ns. (The mean free path against elastic scattering exceeds the size of the crystal at cryogenic temperatures.) These distances must be measured in units of the distance for exponential growth vT_1/n, which for a typical situation with $T_1\sim1$ ms and $n\sim3\times10^5$ amounts to 20 μm. Because the process of stimulated emission depends exponentially on the distance traveled, it is very directional and significant only for a fraction ε of the resonant phonon modes determined by the geometry of the resonant zone and the illuminated pencil (Fig. 1).

When we assume the amplified phonons to travel along

the cylinder axis, i.e., **v** points along the positive x axis for all relevant phonon modes, introduce the quantity $p(x,t)$ as the average $p_{\mathbf{k}}$ for these modes, define the dimensionless quantity

$$n(x,t)=(N_+-N_-)/\rho\Delta\nu \tag{4}$$

to measure the inversion, and finally neglect spontaneous emission as well as radiative decay since they are slow in comparison with the phonon interruption rate n/T_1 and the rate $\varepsilon p/T_1$ of population decay by stimulated emission, then the phonon dynamics is governed by the nonlinear set of equations

$$\frac{\partial p}{\partial t}+v\frac{\partial p}{\partial x}=\frac{np}{T_1}, \tag{5}$$

$$\frac{\partial n}{\partial t}=-\frac{2\varepsilon np}{T_1}. \tag{6}$$

Here, ε is the fraction of the resonant phonons having the appropriate direction, i.e., the solid angle subtended by the resonant phonons taking part in the phonon avalanche divided by 4π. As initial conditions at time $t=0$, we adopt

$$p(x,t=0)=p_0(x), \quad n(x,t=0)=n_0(x). \tag{7}$$

Here, $n_0(x)$ is the initial inversion, created by the optical pumping, and $p_0(x)$ is the initial phonon occupation number, either provided by the minute thermal occupation or created by the heat dissipated by the laser pulse in the bulk of the crystal or at its surfaces. Elimination of n from Eqs. (5) and (6) yields

$$\left(\frac{\partial}{\partial t}+v\frac{\partial}{\partial x}\right)\left(\frac{1}{p}\frac{\partial p}{\partial t}+\frac{2\varepsilon p}{T_1}\right)=0, \tag{8}$$

which can be integrated to

$$\frac{1}{p}\frac{\partial p}{\partial t}+\frac{2\varepsilon p}{T_1}=f(x-vt). \tag{9}$$

Here, the function f is to be determined from the initial conditions, which yields

$$f(x-vt)=\left[-v\frac{d}{d\xi}\ln p_0(\xi)+\frac{n_0(\xi)}{T_1}+\frac{2\varepsilon p_0(\xi)}{T_1}\right]_{\xi=x-vt}. \tag{10}$$

Equation (9) is known as a Bernoulli equation.[14] It can be solved by reducing it to a linear equation by going over to a new variable $q(x,t)=1/p(x,t)$. The general solution of Eqs. (5) and (6) under the initial conditions (7) then reads

$$p(x,t)=p_0(x-vt)\frac{\exp[2\varepsilon P_0(x-vt,x)+N_0(x-vt,x)]}{1+2\varepsilon I_0(x-vt,x)}, \tag{11}$$

$$n(x,t)=\frac{n_0(x)}{1+2\varepsilon I_0(x-vt,x)}, \tag{12}$$

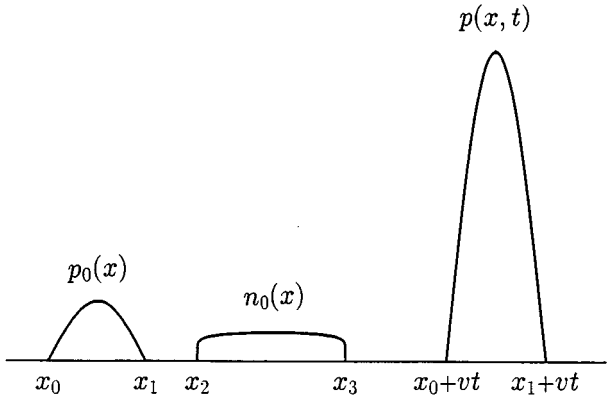

FIG. 2. Visualization of the initial conditions. The initial distribution of phonon occupations $p_0(x)$ is taken nonzero between x_0 and x_1, while the initial resonant inversion $n_0(x)$ is finite between x_2 and x_3. After time t the phonon distribution has moved completely through $n_0(x)$, to become $p(x,t)$. Spatial separation, necessary to derive Eqs. (19) and (20), implies that $x_1<x_2$.

in which the traveling phonon population is reflected in the occurrence of $x-vt$. The quantities P_0, N_0, and I_0 are integrals over space defined by

$$P_0(x',x)=\frac{1}{vT_1}\int_{x'}^{x}p_0(\xi)d\xi, \tag{13}$$

$$N_0(x',x)=\frac{1}{vT_1}\int_{x'}^{x}n_0(\xi)d\xi, \tag{14}$$

$$I_0(x',x)=\frac{1}{vT_1}\int_{x'}^{x}p_0(\xi)\exp[2\varepsilon P_0(\xi,x)+N_0(\xi,x)]d\xi. \tag{15}$$

Note that P_0, N_0, and I_0 are dimensionless. The physical interpretation of $N_0(x',x)$ is the number of initially inverted spins a particular phonon interacts with on its travel from position x' to x. Similarly, $2\varepsilon P_0(x',x)$ is the number of phonons which are initially present between x' and x, and on their travel interact with a given excited center.

Equations (11) and (12) are rigorous solutions when starting from Eqs. (5) and (6). In the event the initial phonon occupation $p_0(x)$ and the initial inversion $n_0(x)$ are disjunct in space, the integral $I_0(x-vt,x)$ occurring in the denominators of Eqs. (11) and (12) can be considerably simplified. The condition of initial separation is visualized in Fig. 2. The initial inversion is taken to be limited to the interval $[x_2,x_3]$. The phonon population is positioned within the interval $[x_0,x_1]$ at time $t=0$, from where it has proceeded to $[x_0+vt,x_1+vt]$ at time t. During its travel the phonon population traverses the initial inversion. Because $p_0(\xi)$ is nonzero only for $\xi<x_1$ and contributions to $N_0(\xi,x)$ arise only from $\xi>x_2$, the part with $N_0(\xi,x)$ in $I_0(x-vt,x)$ can be taken outside the integral upon substituting $N_0(x_2,x)$ for $N_0(\xi,x)$. We thus find $I_0(x-vt,x)$ to become

$$I_0(x-vt,x)=\frac{1}{vT_1}\exp[N_0(x_2,x)]\times\int_{x-vt}^{x}p_0(\xi)\exp[2\varepsilon P_0(\xi,x)]d\xi$$
$$=\frac{1}{2\varepsilon}\exp[N_0(x_2,x)]\times\{\exp[2\varepsilon P_0(x-vt,x)]-1\}, \quad (16)$$

which is rigorous as long as the initial $p_0(x)$ and $n_0(x)$ are separated in space. Inserting this expression into Eqs. (11) and (12) yields after complete passage of the phonon pulse, i.e., for times larger than $t_1=(x_3-x_0)/v$,

$$p(x,t)=p_0(x-vt)\times\frac{\exp[2\varepsilon P_0(x-vt,x_1)+N_0(x_2,x_3)]}{1+\{\exp[2\varepsilon P_0(x-vt,x_1)]-1\}\exp[N_0(x_2,x_3)]}, \quad (17)$$

$$n(x,t)=n_0(x)\frac{1}{1+\{\exp[2\varepsilon P_0(x_0,x_1)]-1\}\exp[N_0(x_2,x)]}. \quad (18)$$

In Eqs. (17) and (18), use has been made of the fact that x must lie between x_2 and x_3 for $n(x,t)$ to be nonzero and between x_0+vt and x_1+vt for a nonzero $p(x,t)$.

An attractive feature of Eqs. (17) and (18) is that they can be integrated exactly to obtain quantities that are directly accessible to experiment, viz., the inversion $N(t)$ and the phonon occupation $P(t)$ at time t integrated over x. That is, by analogy with Eqs. (13) and (14),

$$2\varepsilon P(t)=\frac{2\varepsilon}{vT_1}\int_{x_0+vt}^{x_1+vt}p(x,t)dx$$
$$=N_0(x_2,x_3)+\ln\{\exp[2\varepsilon P_0(x_0,x_1)]-1+\exp[-N_0(x_2,x_3)]\}, \quad (19)$$

$$N(t)=\frac{1}{vT_1}\int_{x_2}^{x_3}n(x,t)dx$$
$$=2\varepsilon P_0(x_0,x_1)-\ln\{\exp[2\varepsilon P_0(x_0,x_1)]-1+\exp[-N_0(x_2,x_3)]\}. \quad (20)$$

The quantities $P(t)$ and $N(t)$ obey energy conservation, as given by the relation

$$2\varepsilon P(t)+N(t)=2\varepsilon P_0(x_0,x_1)+N_0(x_2,x_3). \quad (21)$$

The above formalism is eminently suited for a direct comparison with the experimental results for a phonon pulse that is repetitively amplified by passage through an inverted zone of limited extent. Equations (19) and (20) describe the *integrated* phonon occupation $P(t)$ and population inversion $N(t)$ after a passage of the phonon pulse in terms of these quantities before the passage. Therefore, the output values for $P(t)$ and $N(t)$ can be inserted back into the equations as input for the next passage through the active zone, of course with appropriate allowance in $P(t)$ for any loss the phonon pulse may suffer on its travel as a result of scattering and specular reflection by the end faces of the crystal. The spin population inversion remaining after the previous passage, on the other hand, is not likely to change much. The assumption needed to derive Eqs. (19) and (20), viz., that phonon pulse and inversion are separated in space before their interaction, is, of course, a simplification in the case of the first passage; for later passages the assumption is fully justified. The simplification is plausible, however, because the largest contribution stems from phonons that travel over the full length of the inverted zone, and thus are by far the most amplified.

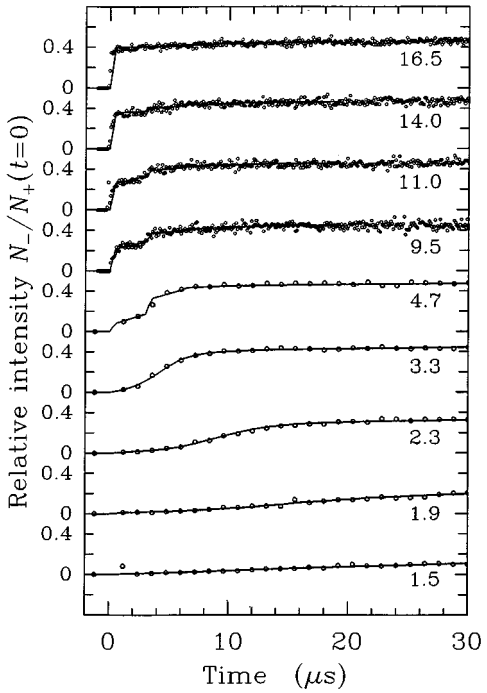

FIG. 3. The growth of N_- normalized to $N_+(0)$ after pumping into E_+ for $H=4$ T and $\theta=69°$. The $E(^2E)$ splitting energy is 1.64 cm^{-1} and $T_1=520$ μs. The labels denote the initial integrated inversion $N_0(x_2,x_3)$. The curves are fits to the data, as described in the text. The occurrence of a phonon cavity is demonstrated by a recurrence in the amplification showing up at intermediate inversions. The upper four traces were taken with a dwell time of 0.1 μs, the lower five traces with a dwell time of 1.2 μs.

IV. RESULTS AND DISCUSSION

A representative selection of the data is collected in Figs. 3–5. Figure 3, which shows the data obtained in a magnetic field $H=4$ T at an angle $\theta=69°$ relative to the crystalline c axis, exemplifies the case of intermediate phonon frequencies and intermediate spin-phonon coupling. For a series of pumping powers, corresponding to values of $N_0(x_2,x_3)$ ranging from 1.5 up to 16.5 as indicated, the population N_- of the lower doublet level E_- is seen to grow with time, the faster the higher the pumping. Note that at the highest initial inversion stimulated emission has accelerated the decay within $E(^2E)$ to a rate exceeding the finite time resolution of the apparatus.

An intriguing effect occurs at intermediate pumping pow-

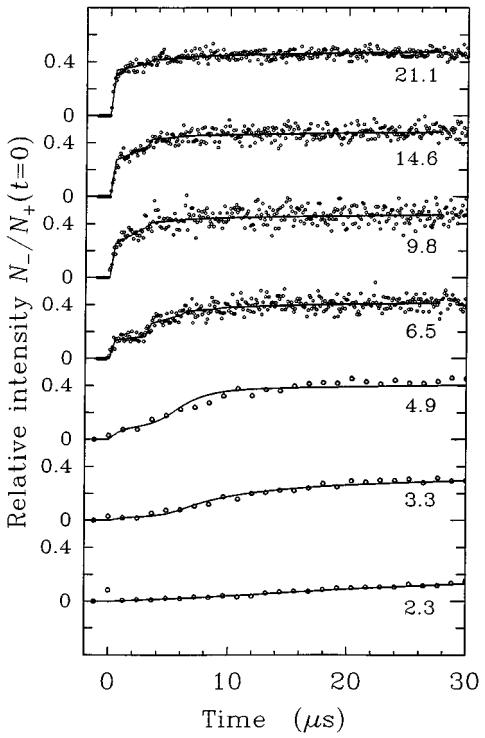

FIG. 4. The growth of N_- normalized to $N_+(0)$ after pumping into E_+ for $H=6$ T and $\theta=80°$. The $E(^2E)$ splitting energy is 1.19 cm^{-1} and $T_1=540$ μs. The labels denote the initial inversion $N_0(x_2,x_3)$. The curves are fits to the data, as described in the text.

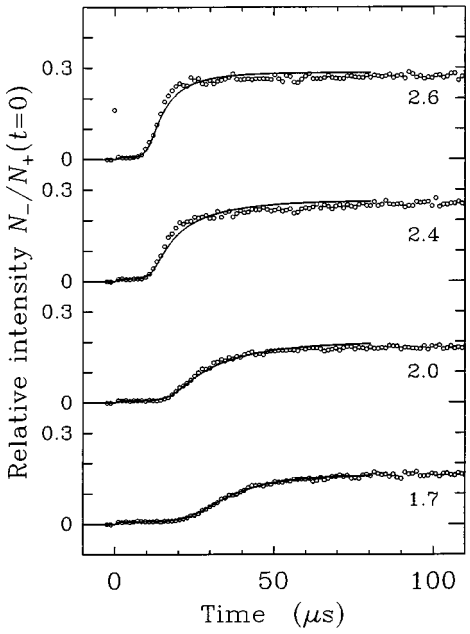

FIG. 5. The growth of N_- normalized to $N_+(0)$ after pumping into E_+ for $H=1.5$ T and $\theta=69°$. The $E(^2E)$ energy splitting is 0.61 cm^{-1} and $T_1=70$ ms. The labels denote the initial inversion $N_0(x_2,x_3)$. The curves are fits to the data, as described in the text. The avalanches with these slow spin-phonon coupling suffer strongly from upconversion because extremely high phonon occupation numbers are reached.

ers, where under suitable conditions a repetitive growth of N_- with time is observed. The time span between successive points of maximal ascent of N_- amounts to 3.3 ± 0.2 μs, which quite remarkably equals twice the time transverse phonons take to cover the distance between the end faces of the crystal (1.7 μs for an 11-mm-long crystal and $v=6.4$ km/s). This is a prominent result of this paper, since it is direct experimental evidence that the crystal forms a phonon cavity. A ballistic phonon pulse travels back and forth between the end faces, and stimulated emission causes enhancement of the spin-lattice relaxation each time the phonons pass through the active zone.

To corroborate this finding, we have repeated these measurements in other magnetic fields for phonon energies ranging from 0.8 to 3.2 cm^{-1} and spin-phonon relaxation times ranging from 34 μs to 16 ms, all with identical results for the period of the recurrence of stimulated emission. An example is shown in Fig. 4. For a more critical check, however, we refer to Fig. 4 of the following paper,[12] in which the growth of N_- is shown as observed in a substantially smaller sample, having a length of 6.0 mm. The period is found to be reduced to 2.0 ± 0.2 μs, which indeed corresponds to the round-trip time of a phonon pulse traveling in a 6-mm-long cavity.

As for the data at the lower pumping powers, also here reflection by the end faces back into the active zone greatly enhances the phonon avalanche. In fact, the avalanche can only become sizable with the assistance of returning phonons. In Fig. 3, this is apparent from the fact that N_- does not start to grow significantly at low pumping powers until the phonons have completed several round trips between the end faces. Again, a highly directional phonon beam is created, which travels back and forth between the end faces and is amplified every time it traverses the resonant inverted zone, until the inversion has fallen to such a low value that stimulated emission fails to overcome the losses. However, the relative slowness of the stimulated process obliterates well-defined points of maximal enhancement, and so no periodicity is observed. For the lowest trace in Fig. 3, detailed analysis shows that the inversion is already inadequate immediately after the pump pulse.

Before carrying out the analysis below, we note that phonon amplification can only be repetitive if it takes place in a volume of limited extent. If the phonons were amplified over the full length of the excited cylinder, no slowdown of the amplification between successive passes would be observed. Macroscopic inhomogeneous broadening of the $E(^2E)$ splitting associated with inhomogeneities in the external field as well as spatial variations in the g factor[13] are obvious causes for spatial confinement of the stimulated emission. Another cause is geometrical effects. Perfect geometry in the sense of no confinement would entail, first, that the group velocity of the amplified phonons is parallel to the axis of the excited zone and, second, that the phase velocity is perpendicular to the reflecting end faces. These conditions are difficult to meet simultaneously in any real situation because of phonon focusing and the particular requirements of the experimental configuration (Sec. II).

A second point is the observation that at higher powers

the growth in N_- speeds up at quite an early instant. This evidences that the initial phonon occupation has the form of an extended ''hot track'' rather than that it is generated by local heating at the surface. Surface heating would involve an appreciable delay in the onset of the amplification that is associated with travel of the generated phonons to locations farther out along the excited pencil.

The third and last point in our discussion of the qualitative characteristics concerns the period between the points of maximum amplification. At first thought, one expects to observe a sizable phonon amplification every time the phonon pulse traverses the part of the active medium it is resonant with. What we instead see is that the period corresponds to the time needed to cover *double* the length of the crystal, i.e., a complete round trip. This is accounted for quite naturally by noting that the phonon distribution leaving the active zone after the first passage is made up of phonon ''packets'' that are resonant with $E(^2E)$ at different locations in the active zone. Following the first reflection by the surface, therefore, each of these phonon packets passes through its resonant location at a distinctly different moment. During the next passage, however, after being reflected by the opposite end face, all packets have covered precisely the same distance when they return to their respective ''native regions.'' For odd-numbered passages, therefore, further phonon amplification is spread out in time, whereas for even-numbered passages it takes place at precisely the same instant. Note in this context that the luminescence is collected by integration over nearly the entire excited zone. It should further be realized that only a small fraction of the initially generated phonons actually return to the active zone because the cone of active phonon modes narrows down after the first specular reflection. This cone is roughly maintained during following reflections. So the amplification following the second and any subsequent reflections affects the inversion more pronouncedly than does the amplification following the first reflection.

On the basis of these considerations we adopt the following model to describe the data. In Sec. III, we have worked out the spatial and temporal dependences of the phonon pulse $p(x,t)$ and the inversion $n(x,t)$, starting from an initial inversion $n_0(x)$ as created by the laser and an initial phonon pulse $p_0(x)$. In addition, we have calculated the spatial integrals $P(t)$ and $N(t)$ of these quantities immediately after the passage, which, on the proviso that the initial phonon pulse and the initial inversion be separated in place, appears to depend on the values of $P(t)$ and $N(t)$ prior to the passage. The final expressions for $P(t)$ and $N(t)$ are given in Eqs. (19) and (20), respectively. Dynamic feedback by returning phonons can thus be incorporated in a natural and simple way by repetitive application of Eqs. (19) and (20). To calculate the amplification of each passage, the initial $P(t)$ and $N(t)$ are set equal to their values prevailing at the moment t_1 the phonon pulse last left the resonant volume with due account of the modifications experienced until the moment t_2 of return. Furthermore, ε is appropriately adjusted.

With regard to ε, it has already been noted that only a small fraction of the phonons generated in the first stage of amplification will induce stimulated emission for a second time. These phonons first have to reflect from a crystalline surface, which reduces the pulse amplitude with the coefficient for specular reflection R. [In the model $P(t)$ and $N(t)$ are calculated after each reflection.] Second, the return path must traverse the active volume (Fig. 1). To model this in a tractable way, we limit the number of phonons modes in the second stage of amplification to a fraction ε' of the total number of modes rather than the fraction ε taking part in the first stage of amplification. For a crystal that, as a case in point, is 10 times longer than the length over which the phonons remain in resonance, ε'/ε amounts to roughly 0.01. We assume that ε' does not alter significantly following the next reflection at the other end of the crystal, and so on. Because ε' is so small, the second stage of amplification tends to produce a lesser change in the inversion than does the first stage, although it further enhances the phonon occupation number. After subsequent reflections, however, the drop of the inversion speeds up again because a sufficiently high number of phonons has built up to compensate for the reduced ε.

To complicate matters, the experiments indicate that phonon loss by upconversion, i.e., the conversion of two resonant phonons into a single one of double the energy by anharmonicity, must be taken into account when high phonon occupation numbers are reached. Upconversion of phonons adds a term proportional to p^2 to the equation of motion for the phonon occupation number, Eq. (1).[10] Its inclusion precludes analytic solution of Eqs. (5) and (6). Since the active zone is confined in space, however, a reasonable approximation is to limit the interaction among the phonons to when they are outside the active zone, so that $n=0$. The analog of Eq. (5) then reads

$$\frac{\partial p}{\partial t}+v\frac{\partial p}{\partial x}=-\frac{p^2}{\tau_a}, \tag{22}$$

in which the time τ_a is a measure for the strength of the anharmonic coupling. The solution of Eq. (22) is

$$p(x,t)=\frac{p_1[x-v(t-t_1)]}{p_1[x-v(t-t_1)](t-t_1)/\tau_a+1}, \tag{23}$$

in which $p_1(x)$ represents the phonon pulse at the time t_1 of its last departure from the active zone. To find the returning phonon pulse, this result is multiplied by R and v is taken to change sign halfway. At the moment t_2 of return, therefore,

$$p(x,t_2)=\frac{p_1(x)}{p_1(x)(t_2-t_1)/\tau_a+1}R. \tag{24}$$

For a square pulse of length l, we have $p(x,t)=P(t)vT_1/l$ over the pulse interval. Because the energy in the phonon pulse is proportional to $2\varepsilon P(t)$, we rewrite the solution to

$$2\varepsilon P(t_2)=\frac{2\varepsilon P(t_1)}{2\varepsilon P(t_1)(t_2-t_1)vT_1/2\varepsilon l\tau_a+1}R, \tag{25}$$

and so the net effect of the anharmonic decay is determined by $\varepsilon l \tau_a$, provided v and T_1 are known.

For the $N(t_2)$ serving as a new initial condition we adopt, in the same spirit, the value reached according to Eq. (20) at t_1, but corrected for spontaneous emission occurring between the phonon passages. Inclusive of this correction, we have

$$N(t_2)=N(t_1)-\frac{t_2-t_1}{T_1}[N_0(x_2,x_3)+N(t_1)], \qquad (26)$$

where the integration boundaries x_2 and x_3 delimit the relevant resonant region.

Upon fitting the model just discussed to the data for $N_-(t)/N_-(0)=[N_0(x_2,x_3)-N(t)]/N_0(x_2,x_3)$ in Figs. 3 and 4, the following combinations of parameters can be derived. On account of Eq. (6), the amplitude of the phonon pulse $P_0(x_0,x_1)$ and the fraction ε of the number of resonant modes, and similarly $P_0(x_0,x_1)$ and ε', appear in the final expressions for $P(t)$ and $N(t)$ only in the form of their product. Related to this point is the fact that the product $\varepsilon' l \tau_a$ is the relevant parameter for the strength of the anharmonic coupling [cf. Eq. (25)]. Accordingly, the adjustable parameters are the products εP_0, $\varepsilon' P_0$, and $\varepsilon' l \tau_a$, the reflection coefficient R, and the proportionality constant $N_0(x_2,x_3)/P$ between the initial inversion and the laser pulse power.

As to the limits of these parameters, ε, ε', and R must, of course, be smaller than unity. The quantity P_0 may correspond to an average temperature that is well above the actual one, because of laser heating and because spontaneously emitted phonons may initiate stimulated emission. On account of the experimental fact that no enhanced relaxation among the $E(^2E)$ levels is observed upon pumping into the lower level, however, an upper limit is about 10 K.[15] The proportionality constant $N_0(x_2,x_3)/P$ depends on the absorption coefficient, the size of the laser focus, the number of resonant phonon modes $\rho\Delta\nu$, and the size of the resonant regions of the crystal. Its value can accordingly be varied to the extent permitted by the uncertainties in these quantities. The full linewidth at half maximum $\Delta\nu$ has been measured in an independent fluorescence line narrowing (FLN) experiment,[13] which yielded the result 95 ± 10 MHz.

To arrive at quantitative results, we have made a single comprehensive fit to the series of traces presented in Fig. 3 and a similar fit to the data in Fig. 4. The parameters $\varepsilon' l \tau_a$, R, and $N_0(x_2,x_3)/P$ were assumed to be the same for all traces, but εP_0 and $\varepsilon' P_0$ were allowed to vary from trace to trace. The drawn curves in Figs. 3 and 4 represent the model with the fitted parameters inserted. As is apparent from these figures, there is good agreement with the experiment. Particularly noteworthy is that the recurrence of the amplification is faithfully reproduced. For the reflection coefficient we found from the data in Fig. 3 the result $R=0.23\pm0.05$, which is quite reasonable for phonons of this wavelength in consideration of the quality of the surfaces.[16] For the top trace in Fig. 3, for example, we found $\varepsilon P_0\approx 2\times10^{-3}$ and $\varepsilon' P_0\approx 4\times10^{-5}$. Finally, the fit yielded the result $\varepsilon' l \tau_a = 120\pm20$ cm μs. It is difficult to quantify ε, ε', and τ_a separately, because we have no knowledge of the initial phonon occupation and the phonon pulse length.

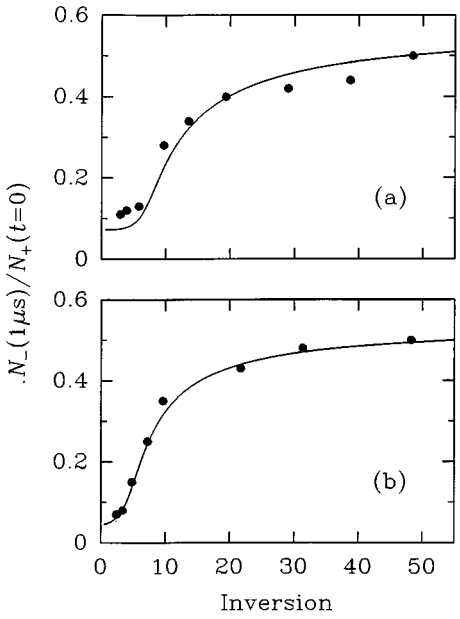

FIG. 6. N_- normalized to $N_+(0)$ at 1 μs after pumping E_+ as a function of the initial inversion, $N_0(x_2,x_3)$. (a) $H=6$ T and $\theta=30°$, (b) $H=6$ T and $\theta=62°$. The curves are fits to the data, as described in the text.

As an upper limit for the latter, we have $\sim$500 ns from the lead time of the fastest parts of the amplification. With this value, we find $l\approx3$ mm. If for the upper trace in Fig. 3 the phonon temperature is somewhat arbitrarily assumed to be 10 K, corresponding to $P_0=4\times10^{-3}$, the quantities ε and ε' are deduced to be of order 0.5 and 0.01. For the strength of the anharmonic coupling we then arrive at $\tau_a\sim40$ ms. For the data in Fig. 4, we similarly find $R=0.15\pm0.05$, $\tau_a\sim60$ ms, and values for the other parameters comparable to those found from Fig. 3.

No recurrence of the amplification was observed at high phonon energies, i.e., δ between 3.2 and 6.0 cm^{-1}, which at $H=6$ T is reached for θ ranging from 30° to 62° (Fig. 6). These conditions correspond to relaxation times T_1 between 15 and 34 μs. One reason for this is that the excited zone is at an unfavorable angle with respect to the crystalline faces, so that phonons amplified parallel to the excited cylinder are not reflected back into the excited zone. Second, at these frequencies R may be diminished because the surface roughness is of the order of the phonon wavelength. The phonon avalanche then takes place well within the first μs. It cannot be resolved in time with the present technique owing to the small number of photomultiplier counts collected. For this reason, we have, by analogy with the treatment in Ref. 10, considered the change in N_- accumulated during the first 1 μs, i.e., the effect of a completed avalanche, as a function of the initial inversion (Fig. 6). To analyze these data, the change in the inversion as given by Eq. (20) was fitted to the observed change in N_- that results after a *single* passage of the phonon pulse. Note here that a full round trip of a phonon lasts 3.3 μs. Also note that within the model this leaves us with only two adjustable parameters, viz., εP_0 and the proportionality constant $N_0(x_2,x_3)/P$. No value for τ_a has been

derived since upconversion was assumed ineffective during the phonon passage. This is certainly adequate here because the fraction of active phonon modes is still high, and the phonon occupation numbers needed to account for the observed increase of the relaxation rate are relatively low. As it appears, the fitted curve satisfactorily tracks the data in Fig. 6 for the value of εP_0 corresponding to an average initial phonon temperature of approximately 10 K ($\varepsilon \approx 0.5$). The same analysis was done, with similar conclusions, for the other series at high phonon energies.

We next discuss stimulated emission of low-energy phonons. Figure 5 shows the results for $\delta = 0.61$ cm^{-1} and $T_1 \approx 70$ ms. At this energy, spin-phonon coupling is so weak that stimulated emission is inherently slow in comparison with the phonon round-trip time (3.3 μs). The conditions for a periodicity in the amplification are accordingly not met. Furthermore, substantial optical pumping powers are needed to provide reasonable inversions. By contrast to the cases of intermediate and high phonon energies, stimulated emission appears to start up not immediately following heating by the laser pulse, but after a delay of order 10 μs or more, presumably by spontaneously emitted phonons as well as thermal ones. This again is indicative of the reflection of generated phonons by the crystal faces back into the active zone, because the avalanche can only take such a long time to develop if the phonons are not lost after their flight to a surface.

We have therefore fitted the same model as used above to the low-energy data of Fig. 5. As it turned out, a satisfactory fit could not be made but with the inclusion of anharmonic upconversion. This is particularly noteworthy because at these low phonon energies upconversion is quite inefficient. Apparently the phonon occupation numbers reached are so extreme that they easily offset the inefficiency of the scattering process. The cause for high phonon occupations, in turn, resides in the fact that the heat capacity of the spin system is so large relative to that of the resonant phonons. To illustrate this, in the uppermost trace of Fig. 5 the time constant of the avalanche is of the order of 7 μs, compared to $T_1 = 70$ ms. So $\varepsilon' p$ is of order 10^4, yielding p's of order 10^6.

As for the adjusted parameters, R is anticipated to depend strongly on the properties of the surface and to decrease with increasing energy. The surfaces of our crystal were polished down to a roughness of 0.1 μm, i.e., the wavelength of 2-cm^{-1} phonons. Indeed, this frequency is of the order of the upper limit (3.2 cm^{-1}) for which recurrence of the emission was observed. With regard to the products εP_0 and $\varepsilon' P_0$, the quantities $\varepsilon \sim 0.5$ and $\varepsilon' \sim 0.01$ are primarily determined by the geometry and therefore are comparable for all runs. The quantity P_0, on the other hand, varies from trace to trace with the power of the laser pulse, but, as already noted, quite modest initial phonon temperatures up to about 10 K provided satisfactory fits of the model. In Fig. 7, the results for $\varepsilon' l \tau_a$ as derived from all data are collected as a function of the phonon energy δ. To the extent ε' and l are constants, $\varepsilon' l \tau_a$ represents the frequency dependence of the anharmonic coupling. From theoretical considerations[17] as well as by analogy with other experiments,[18,19] a dependence according to δ^{-5} is expected. However, if the anharmonic decay is restricted to the energy interval of the resonant phonons, the energy dependence is rather given by

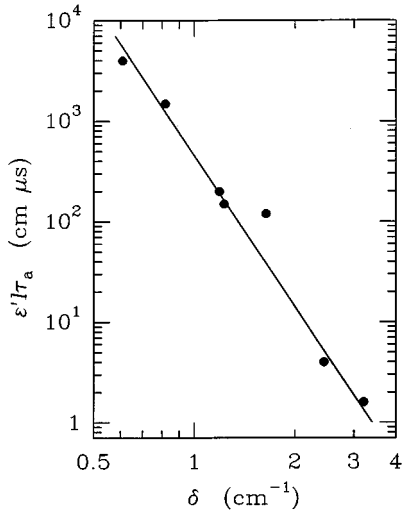

FIG. 7. The anharmonic decay strength, expressed in $\varepsilon' l \tau_a$, as a function of phonon energy. The solid curve is a δ^{-5} dependence on the $E(^2E)$ level splitting δ.

$(\delta^4 \Delta\delta)^{-1}$,[20] in which $\Delta\delta$ is the linewidth of the transition. This would result in a δ dependence somewhere between δ^{-4} and δ^{-5}, since $\Delta\delta$ is known to increase to some extent with δ,[13] and l presumably decreases slightly with δ.

V. CONCLUSIONS

We have demonstrated amplified stimulated emission of phonons in an acoustical cavity formed by a crystal. This, of course, is a first step toward constructing a phonon laser. The phonon avalanches were generated by optical pumping into the upper component of a magnetic-split Kramers doublet and detected via the associated enhancement of the spin-lattice relaxation. The evidence for the phonon cavity is a repetitive recurrence of the relaxation with a period equal to the flight time for a round trip of transverse phonons via the end faces of the crystal. The end faces thus act as mirrors, which reflect part of the phonons back into the active zone and which give rise to repeated amplification by stimulated emission. The model used is based on rate equations with inclusion of phonon migration, which are solved rigorously under the simplifying assumption that initial phonon occupation $p_0(x)$ and the initial inversion $n_0(x)$ are disjunct in space. The effects of successive single passes through the active zone are compounded to provide a faithful description of the development of the avalanches. At low phonon energies, for which very high phonon occupation numbers are reached, nonlinear phonon loss, such as provided by anharmonic upconversion, must be taken into account.

ACKNOWLEDGMENTS

The work was supported by the Netherlands Foundation Fundamenteel Onderzoek der Materie (FOM) and the Nederlandse Organisatie voor Wetenschappelijk Onderzoek (NWO).

[1] Preliminary conference reports of this work are P. A. Fokker, J. I. Dijkhuis, and H. W. de Wijn, J. Lumin. **53**, 35 (1992); in *Phonon Scattering in Condensed Matter VII*, edited by M. Meissner and R. O. Pohl, Springer Series in Solid State Sciences Vol. 112 (Springer-Verlag, Berlin, 1993), p. 114.
[2] E. B. Tucker, Phys. Rev. Lett. **6**, 547 (1961).
[3] William J. Brya and Peter E. Wagner, Phys. Rev. Lett. **14**, 431 (1965); Phys. Rev. **157**, 400 (1967).
[4] W. B. Mims and D. R. Taylor, Phys. Rev. Lett. **22**, 1430 (1969); Phys. Rev. B **3**, 2103 (1971).
[5] E. M. Ganapol'skii and D. N. Makovitskii, Sov. Phys. JETP **45**, 106 (1977).
[6] W. E. Bron and W. Grill, Phys. Rev. Lett. **40**, 1459 (1978).
[7] P. Hu, Phys. Rev. Lett. **44**, 417 (1980).
[8] D. J. Sox, J. E. Rives, and R. S. Meltzer, Phys. Rev. B **25**, 5064 (1982).
[9] M. H. F. Overwijk, J. I. Dijkhuis, and H. W. de Wijn, Phys. Rev. Lett. **65**, 2015 (1990).
[10] J. G. M. van Miltenburg, G. J. Jongerden, J. I. Dijkhuis, and H. W. de Wijn, in *Phonon Scattering in Condensed Matter*, edited by W. Eisenmenger, K. Lassmann, and S. Döttinger (Springer-Verlag, Berlin, 1984), p. 130.
[11] J. I. Dijkhuis, K. Huibregtse, and H. W. de Wijn, Phys. Rev. B **20**, 1835 (1979).
[12] P. A. Fokker, R. S. Meltzer, Y. P. Wang, J. I. Dijkhuis, and H. W. de Wijn, following paper, Phys. Rev. B **55**, 00000 (1997).
[13] P. A. Fokker, R. J. E. Jaspers, J. I. Dijkhuis, and H. W. de Wijn (unpublished).
[14] See, e.g., Earl D. Rainville, *Elementary Differential Equations* (Macmillan, New York, 1949).
[15] This finding also justifies the neglect of Orbach relaxation connecting the $E(^2E)$ levels via $2A(^2E)$. Orbach relaxation becomes operative above about 5 K [S. Geschwind, G. E. Devlin, R. L. Cohen, and S. R. Chinn, Phys. Rev. **137**, A1087 (1965)], but the relevant phonons, having an energy of 29 cm^{-1}, escape from the active zone within 30 ns.
[16] G. A. Northrop and J. P. Wolfe, Phys. Rev. Lett. **52**, 2156 (1984).
[17] R. Orbach and L. A. Vredevoe, Physics **1**, 91 (1964).
[18] R. Baumgartner, M. Engelhardt, and K. F. Renk, Phys. Rev. Lett. **47**, 1403 (1981).
[19] W. A. Tolbert, W. M. Dennis, and W. M. Yen, Phys. Rev. Lett. **65**, 607 (1990).
[20] J. G. M. van Miltenburg, Ph.D. thesis, Utrecht University, 1984, Chap. 2.